VIII MEASUREMENTS OF TOTAL COLLISION CROSS SECTION FOR DIMERS OF SIMPLE ATOMS AND MOLECULES IN THE GLORY- AND TRANSITION REGION.

VIII.1. INTRODUCTION.

In this communication we present a survey of total collision cross sections for van der Waals dimers of the inert gases Ar and Ne, the molecules H_2, N_2, NO, O_2, CO_2, and C_2H_4, and for mixed dimers NeAr, HeNe and H_2Ar. Most of the measurements of the dimer cross sections, σ_2, relative to the corresponding monomer cross section, σ_1, have been described before (ref. 1, 2, 3, ch. III, IV and VII). For a complete review, we have added the results for the He trimer (ref. 4, ch.V) and our unpublished results for the CO_2 and C_2H_4 dimers.

The dimers are produced in a nozzle beam and are detected by a mass spectrometer. The total collision cross section is determined from the attenuation of the beam by a target gas (Ar, Kr or He) in a scattering chamber (at 80K for Ar and He, 200K for Kr).

In fig. VIII.1 all ratios σ_2/σ_1 are collected and plotted vs. the reduced velocity $v_{red} = \hbar v/\varepsilon R_m$. For mixed dimers the average value of both monomer cross sections is taken instead of σ_1. The systems investigated are summarized in table VIII.1. The relative scattering velocity v is calculated by $v = (v_1^2 + \alpha_s^2)^{1/2}$ (cf. ref. 5); for the beam velocity v_1 full isentropic expansion is assumed (ref. 6); the velocity α_s is the thermal velocity of the target molecules in the scattering chamber. The f.w.h.m. spread in relative velocity is about equal to αs.

The values for ε and R_m are taken from a Lennard Jones interaction potential of monomer (the heavier monomer for mixed dimers) and target molecules (ref. 7, see table VIII.1).

A correction to σ_2/σ_1 for the finite angular resolution is applied following ref. 8. The absolute value of the total cross section, required for the calculation of the correction, is determined from Swedenburg et al. (ref. 9) and Gengenbach et al. (ref. 10), and our relative measurements.

The correction formula of ref.8 has been derived under the assumptions $v_1/\alpha_s \geq 2$ and $\sigma_1 \propto v^{-2/5}$. Consequently, this correction is uncertain for He as target molecule. Due to lack of a better procedure, it is applied, nevertheless. The fact that the experimental results taken with He in the scatterbox do not show any striking deviation in fig. VIII.1 has helped us to subdu[illegible] scruples. In table VIII.1 both measured and corrected values of σ_2/σ_1 ar[illegible] given.

Because of the large spread in relative velocity we do not observe a glory type velocity dependence of σ_2/σ_1. The monomers and dimers in the beam have essentially the same velocity. The spread in relative velocity is pratically entirely due to the thermal velocity of the target gas α_s; the correction factor for the total collision cross section to deal with this spread is equal for both monomers and dimers, leaving the ratio σ_2/σ_1 unchanged.

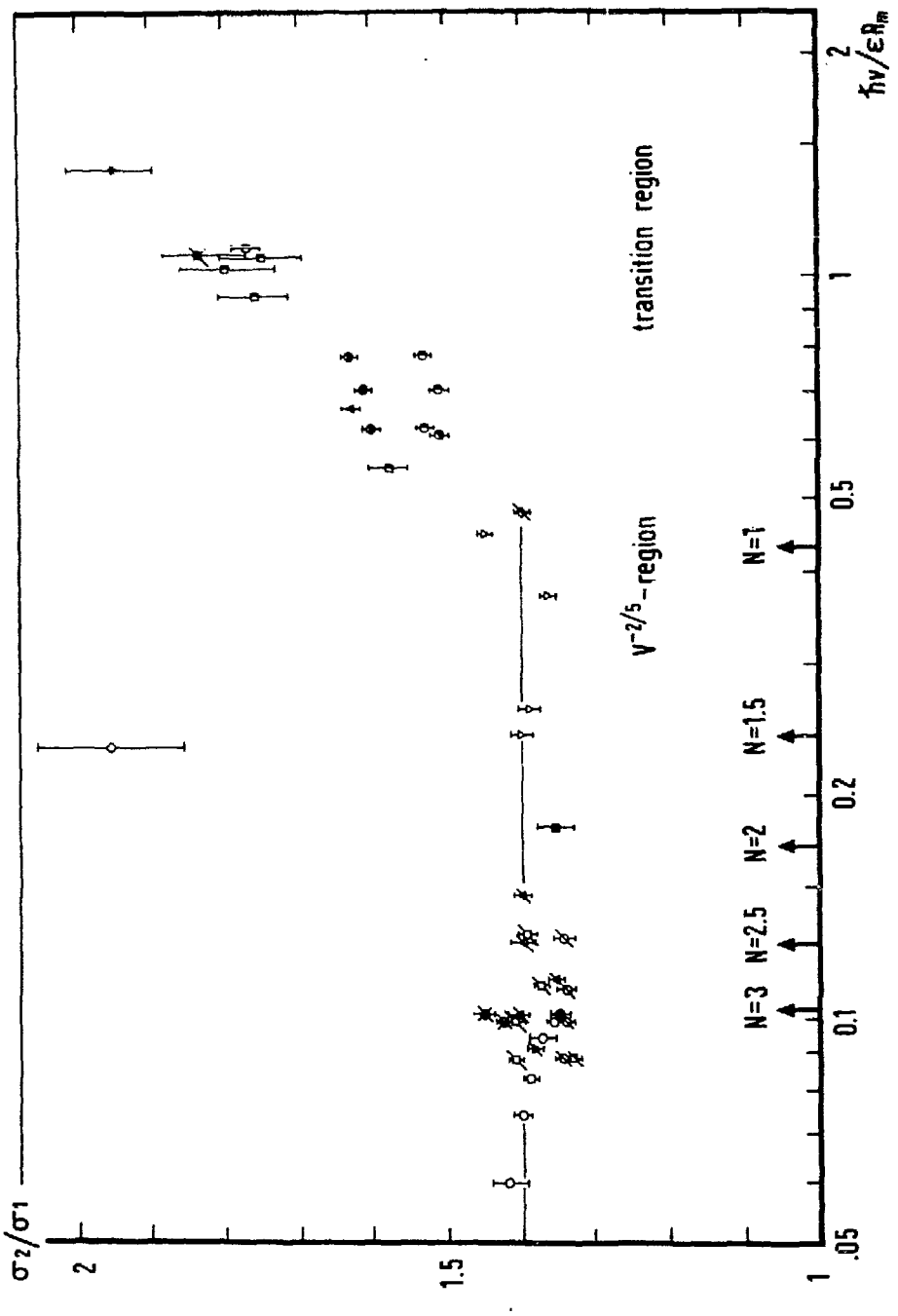

Fig. VIII.1. Cross section ratio σ_2/σ_1 vs. reduced velocity.
The explanation for the symbols corresponding to the different systems is given in table VIII.1.

TABLE VIII.1

Beam	symbol	T_b (K)	v_t (m/sec)	scatter gas	α_a (m/sec)	v (m/sec)	σ_2/σ_1 eff.	ΔC_γ	σ_2/σ_1 corr.	$\hbar v/\varepsilon R_m$	ref.
Argon	○	294	553	Ar	182	582	1.34±.03	1.024	1.37±.03	.093	a
		223	481	Ar	182	515	1.36±.02	1.022	1.39±.02	.083	a
		173	424	Ar	182	462	1.37±.02	1.019	1.40±.02	.074	a
		123	358	Ar	182	401	1.40±.04	1.016	1.42±.04	.057	a
Argon in Ne-Ar (3 : 1)	◔	294	699	He	577	907	1.45±.02	< 1.052 >	< 1.53±.02 >	.78	b
		210	591	He	577	826	1.44±.02	< 1.050 >	< 1.51±.02 >	.70	b
		120	447	He	577	730	1.45±.02	< 1.052 >	< 1.53±.02 >	.62	b
	○	210	591	Ar	182	618	1.28±.02	1.063	1.36±.02	.099	a
Argon in H_2-Ar (8 : 1)	●	90	776	Kr	204	802	1.27±.02	1.059	1.35±.02	.10	f
Neon	◧	100	456	He	577	735	1.72±.02	< 1.026 >	< 1.77±.02 >	1.09	b
		65	368	He	577	684	1.75±.06	< 1.028 >	< 1.80±.06 >	1.02	b
		33	264	He	577	634	1.71±.04	< 1.036 >	< 1.77±.04 >	.94	b
	■	100	456	Kr	204	500	1.30±.05	1.036	1.35±.05	.18	c
Neon in He-Ne (3 : 1)	◧	31	402	He	577	703	1.71±.06	< 1.026 >	< 1.75±.06 >	1.05	b
He	◇	7	270	Ar	182	326	1.95±.10	1.008	1.97±.10	.24	b
H_2	▽	166	1858	Ar	182	1867	1.54±.04	1.007	1.55±.04	.58	b
		100	1442	Ar	182	1453	1.44±.04	1.006	1.45±.04	.44	b
		65	1163	Ar	182	1177	1.35±.02	1.005	1.36±.02	.37	b
		30	790	Ar	182	810	1.38±.03	1.004	1.39±.03	.26	b
		26	736	Ar	182	758	1.40±.03	1.002	1.40±.03	.24	b
	▼	26	736	He	577	929	1.91±.06	< 1.025 >	< 1.96±.06 >	1.38	e
N_2	⊀	294	782	Ar	182	803	1.33±.02	1.053	1.40±.02	.146	f
		220	676	Ar	182	700	1.34±.03	1.046	1.40±.03	.127	f
		173	600	Ar	182	626	1.30±.02	1.041	1.35±.02	.113	f
		133	526	Ar	182	557	1.35±.03	1.042	1.41±.03	.101	f
	⊀	173	600	He	577	832	1.57±.02	< 1.045 >	< 1.64±.02 >	.66	d
NO	⌀	294	756	Ar	182	777	1.27±.03	1.055	1.34±.03	.127	f
		220	654	Ar	182	678	1.27±.02	1.046	1.33±.02	.110	f
		173	580	Ar	182	607	1.29±.02	1.042	1.34±.02	.099	f
		133	508	Ar	182	540	1.29±.02	1.041	1.34±.02	.088	f
	⌀	173	580	He	577	818	1.45±.02	< 1.041 >	< 1.51±.02 >	.61	d
O_2	⌀	294	732	Ar	182	754	1.32±.03	1.055	1.39±.02	.127	f
		220	633	Ar	182	659	1.32±.02	1.049	1.38±.02	.111	f
		173	561	Ar	182	590	1.35±.02	1.046	1.41±.02	.099	f
		133	492	Ar	182	525	1.35±.02	1.042	1.41±.02	.088	f
	◧	133	492	He	577	758	1.51±.05	< 1.041 >	< 1.57±.05 >	.55	d
CO_2	⌀	294	707	Ar	182	730	1.28±0.2	1.035	1.33±.02	.087	f
	◆	294	707	He	577	912	1.33±.02	< 1.050 >	< 1.40±.02 >	.48	d
C_2H_4	⊀	294	782	Ar	182	802	1.32±.02	1.039	1.37±.02	.091	f
Mixed dimers											
NeAr (3 : 1)	⊠	294	699	He	577	907	1.58±.02	< 1.03>	< 1.63±.02 >	.78	b
		210	591	He	577	826	1.56±.02	< 1.03>	< 1.61±.02 >	.70	b
		120	447	He	577	730	1.55±.02	< 1.03 >	< 1.60±.02 >	.62	b
	⊠	210	591	Ar	182	618	1.39±.02	< 1.04 >	1.45±.02	.099	a
HeNe (3 : 1)	⊠	31	402	He	577	703	1.79±.06	< 1.02 >	< 1.83±.06 >	1.05	b
H_2Ar (8 : 1)	✱	90	776	Kr	204	802	1.40±.02	1.04	1.45±.02	.10	f

Table VIII.1. Summary of all dimer to monomer cross section ratios investigated. In the second column the symbols are given which are used in fig. VIII.1 for the different systems. In column σ_2/σ_1 (eff.) the measured ratio of dimer to monomer cross section is displayed; these values have to be multiplied by the correction factor ΔC_γ and σ_2/σ_1 (corr.) to obtain the corrected σ_2/σ_1. For the bracketed values of ΔC_γ and σ_2/σ_1 (corr.) the correction is uncertain. The column $\hbar v/\varepsilon R_m$ gives the reduced velocity, with εR_m values for a from ref. 7a, b from ref. 7b, c from ref. 7c, d from ref. 7d, e from ref. 10, and f from combination rules applied to the ε and R_m values from ref. 7a.

le VIII.1.

Fig.VIII.1 shows that at low reduced velocities $v_{red} < .4$, the ratio σ_2/σ_1 assumes values between 1.32 and 1.45, it rises at larger reduced velocities and approaches a value 2 for $v_{red} > 1$. All σ_2/σ_1 results for the large variety of very different systems fall on one single curve in good approximation. Only He forms a striking exception.

For $v_{red} < .4$ the monomer cross section σ_1 is dominated by attractive forces between monomer and target: With an interaction potential V, $V(r) = -C_{6,m}/r^6$, one has $\sigma_1 = 8.083(C_6/\hbar v)^{2/5}$ (ref.11). When we assume that a similar potential, $-C_{6,d}/r^6$, describes the interaction between dimer and target molecule the ratio σ_2/σ_1 varying from 1.32 to 1.45 points to $C_{6,d}/C_{6,m}$ between 2.0 and 2.5.

Indicated in fig.VIII.1 are the approximate reduced velocities at which glory maxima (integer N) or glory minima (half integer N) would occur in the monomer total collision cross section (ref.12). It is improbable that a loosely bound dimer will survive collisions at glory impact parameters; an eventual glory structure in σ_2/σ_1 will be predominantly due to glories of σ_1.

No distinct glory structure is observed in σ_2/σ_1; the absence can be explained by the velocity averaging in our experimental set up, by the achieved accuracy for σ_2 and the smallness of the glory amplitude. For the H_2-beam and Ar as target, however, a slight variation of σ_2/σ_1 at $.23 < v_{red} < .58$ is observed, which may be attributed to the N = 1 glory of σ_1.

For $v_{red} > .8$ (transition region) the repulsive forces determine the monomer cross section. At high reduced velocities, where the "collision diameter" of the constituent monomer becomes comparable to or smaller than the mean distance in the dimer, we expect $\sigma_2/\sigma_1 = 2$.

The ratio σ_2/σ_1 for NO is slightly but significantly lower than for most other systems. This might be attributed to a strong interaction (of chemical nature or due to dipole-dipole forces) between the two NO molecules in the dimer, which decreases the size of the dimer (ref. 13).

A special case is formed by He; for the smallest He-cluster we find a cross section which is 1.95 times the monomer cross section, although the velocity is well within the $v^{-2/5}$-region, $v_{red} = .23$ (Ar as target). This high ratio is one of the arguments by which we have concluded that the smallest cluster observed for He must be a trimer (ref.4).

1. A. van Deursen, A. v. Lumig and J. Reuss, Int. J. Mass Spectrom. Ion Phys., *18* (1975) 129
2. A. van Deursen and J. Reuss, to be published, ch. IV of this thesis
3. A. van Deursen and J. Reuss, to be published, ch. VII of this thesis
4. A. P. J. van Deursen and J. Reuss, J. Chem. Phys., *63* (1975) 4559
5. R. B. Bernstein, Comments At. Mol. Phys., *4* (1973) 43
6. J. B. Anderson and J. B. Fenn, Phys. Fluids, *8* (1965) 780
7. a/ J. O. Hirschfelder, C. F. Curtiss and R. B. Bird, "Molecular theory of gases and liquids", Wiley, New York (1965)
   b/ R. Helbing, W. Gaide and H. Pauly, Z. Physik, *208* (1968) 215
   c/ B. N. Srivastava and K. P. Srivastava, J. Chem. Phys., *30* (1969) 984
   d/ H. Vehmeyer, thesis, Bonn (1970)
8. F. v. Busch, Z. Physik, *193* (1966) 412
   F. v. Busch, H. J. Strunck and Ch. Schlier, Z. Physik, *199* (1967) 518
9. R. L. Swedenburg, J. A. Phipps, J. E. Scott, Report AEEP-3442-102-70 U, University of Virginia (1970)
10. R. Gengenbach and Ch. Hahn, Chem. Phys., L *15* (1972) 604
11. L. D. Landau and E. M. Lifshitz, "Quantum Mechanics", Pergamon Press, London (1959)
12. R. E. Olson and R. B. Bernstein, J. Chem. Phys., *49* (1968) 162
13. P. N. Skancke and J. E. Boggs, Chem. Phys., L *21* (1973) 316

APPENDIX

A1. VIBROTOR LEVELS OF DIMERS

In table A1.1 the vibrational levels $\varepsilon_{v,0}$ and rotational constants B_v for Ar_2 are shown, taken from Docken and Schafer (ref. A1). The vibrotor levels $\varepsilon_{v,j}$ are given within an accuracy for $\varepsilon_{v,j}/k$ of .2 K (ref.A1) by

$$\varepsilon_{v,j} = \varepsilon_{v,0} + B_v . j.(j+1) \qquad (A1.1)$$

Because ^{40}Ar has a nuclear spin I = 0, it behaves like a boson and only even values of j are allowed (see ref. A2). For each vibrational level the largest j value, $j_{v,max}$, for which a bound state occurs ($\varepsilon_{v,j} < 0$) is given in column 4. Alternatively, we calculated the $\varepsilon_{v,0}$ levels for a Lennard Jones 12-6 (L.J.)

table A1.1

	Ar		
v	$-\varepsilon_{v,0}/k$ (K)	B_v/k (K)	$j_{v,max}$
0	120.1	.083	36
1	83.4	.087	32
2	54.4	.069	26
3	32.7	.062	22
4	17.4	.052	16
5	7.8	.042	12
6	2.6	.030	8
7	.46	.017	4
8	.004	.003	0

Table A1.1 Vibrational levels and rotational constants for Ar_2 from ref A1. The well depth ε/k = 140.8 K.

interaction potential $V(r) = \varepsilon \{(R_m/r)^{12} - 2(R_m/r)^6\}$ in first order J.W.K.B. approximation by solving the $\varepsilon_{v,0}$ values with j = 0 for which v assumes integer values in

$$v + .5 = 2 m_1^{1/2}/h \int_{r_0}^{r_1} [\varepsilon_{v,j} - V(r) - \frac{h^2 j(j+1)}{m_1 r^2}]^{1/2} dr \qquad (A1.2)$$

Here r_0 and $r_1 > r_0$ are the two zero points of the integrand; m_1 stands for the monomer mass. It is convenient to write eq. A1.2 in a reduced form

$$v + .5 = 2/\Lambda^* \int_{r_0^*}^{r_1^*} [\varepsilon^*_{v,0} - V^*(r^*) - \frac{\Lambda^{*2} j(j+1)}{4 r^{*2}}]^{1/2} dr^* \qquad (A1.3)$$

where $r^* = r/R_m$, $r_0^* = r_0/R_m$, $r_1^* = r_1/R_m$, and $\varepsilon^*_{v,j} = \varepsilon_{v,j}/\varepsilon$, $V^*(r^*) = r^{*12} - 2r^{*6}$. The quantity Λ^* stands for the reduced de Broglie wavelength† $\Lambda^* = h/R_m (m_1 \varepsilon)^{1/2}$. With j = 0 the integral in eq. A1.3 is independent of Λ^* and the $\varepsilon_{v,0}$ values depend linearly on $1/\Lambda^*$.

For Ar_2 the reduced $\varepsilon^*_{v,j}$ from the L.J. potential with parameters ε and R_m of ref. A3, are within 1% equal to the $\varepsilon_{v,0}/\varepsilon$ values from ref. A1. Therefore, the $\varepsilon_{v,0}$ values given in table A1.1 are reproduced by our L.J. approximation if we increase at constant $\Lambda^* = .166$ the well depth ε of the L.J. potential, $\varepsilon/k = 124$ K, to the one from ref A1, $\varepsilon/k = 140.8$ K.

By applying eq. A1.3 one can obtain $\varepsilon_{v,j}$ for j = 0 too; however, we aproximate $\varepsilon_{v,j}$ for the L.J. potential according to eq. A1.1 with $B_v = B$ for all vibrational levels. The rotational constant B is taken at the equilibrium distance of the dimer, $B = \hbar^2/m_1 R_m^2$. This approximation yields a value for the partition function Z_2 about 15% too small at maximum.

For ^{20}Ne the vibrational levels $\varepsilon_{v,0}$ and rotational constants B_v are displayed in table A1.2 taken from the discussion of Tanaka et al. (ref. A4) of UV absorption measurements and their comparison to differential cross section measurements by Siska et al. (ref. A5).

The interaction potential of $(H_2)_2$ does support only the j = 0 and j = 1 state, with v = 0. The energies $\varepsilon_{0,j}$ given in table A1.2 are calculated for a L.J. potential with $\Lambda^* = 1.54$, by directly solving the radial Schrödinger equation for the H_2 dimer (ref. A6).

We calculated the vibrational levels $\varepsilon_{v,0}$ for N_2 and NO using eq. A1.3 with $\varepsilon/k = 91.5$K, $R_m = 4.132$ Å, $\Lambda^* = .209$ and $\varepsilon/k = 119$K, $R_m = 3.90$Å, $\Lambda^* = .188$, respectively. These values for ε and R_m are taken from the force constants detemined from viscosity data given in ref. A3. Also indicated in table A1.3 are

† A definition for Λ^* used by other authors (see e.g. ref. A3) involves the finite zero point of the potential σ, instead of R_m. The resulting value for a L.J. potential is a factor $2^{1/6}$ larger than the one from our definition.

the maximum rotational quantum number $j_{v,max}$ using a rotational constant $B = \hbar^2/m_1 R_m^2$, $B/k = .101$K for N_2, $B/k = .105$ K for NO. In the calculation of the partition function Z_2 the monomer rotational constants B_a are taken from ref. A7, for N_2 $B_a/k = 2.88$ K and for NO $B_a/k = 2.44$ K.

For the mixed dimer NeAr the $\varepsilon_{v,0}$ are similarly calculated for a L.J. potential using parameters $\varepsilon/k = 65$ K, $R_m = 3.46$ Å, (ref. A8), $A^* = h/R_m(2\mu\varepsilon)^{\frac{1}{2}} = .30$ where μ is the reduced mass. The $\varepsilon_{v,0}$ value thus found, could be compared to the levels calculated from a more refined potential (see ref. A9). The small effect found for Ar did not seem to justify this effort.

table A1.2

	^{20}Ne			H_2	
v	$-\varepsilon_{v,0}/k$ (K)	B_v/k (K)	$j_{v,max}$	j	$-\varepsilon_{0,j}/k$ (K)
0	25.3	.23	9	0	3.7
1	4.3	.14	5	1	1.4
2	.14	.06	1		

Table A1.2 Vibrational levels and rotational constants for ^{20}Ne, from ref A4; the well depth $\varepsilon/k = 46$K.
Rotational levels for H_2, from ref. A6; the well depth $\varepsilon/k = 34$ K, $A^* = 1.54$.

table A1.3

	N_2		NO	
v	$-\varepsilon_{v,0}/k$ (K)	$j_{v,max}$	$-\varepsilon_{v,0}/k$ (K)	$j_{v,max}$
0	75	23	99	26
1	48	18	66	21
2	28.1	14	40.5	16
3	14.5	10	22.6	12
4	6.0	6	10.7	8
5	1.8	3	3.6	4
6	.14	0	.83	2
7	–	–	<.1	0

Table A1.3 Approximate vibrational levels for N_2 and NO for a L.J. 12-6 potential, and maximum allowed quantum number for the end-over-end rotation.

table A2.1

	1	2	3	4	5a	5b
H_2	.28	.28	.39	.28	.30 ± 3%	.35 ± 3%
He	.094	.10	.13	.14	.134 ± 2%	.134 ± 3%
Ne	.21	.24	.20	.22	.258 ± 2%	.230 ± .3%
Ar	1	1	1	1	1	1
Kr	1.25	1.32	1.56		1.34 ± 2%	1.36 ± 2%
Xe	2.1	2.27	2.29			
N_2,NO,O_2	.77	.82	.84	.67		
CO_2					.90 ± 3%	1.01 ± 3%

Table A2.1 Relative ionization cross sections at electron energies 100 and 130 eV (column 1 and 2, see ref. A.10). In column 3, 4, and 5 the relative efficiencies are given for ionization gauges from ref.A 12a, b, and c; 5a and 5b correspond to different modern gauges, see ref. A11c.

A2. IONIZATION CROSS SECTIONS AND DETECTION EFFICIENCY

In order to compare the monomer intensities for the mixed gases we have tabulated some ionization cross sections with respect to the one of Ar. The electron energies used in the experiment are 100 and 130 eV; in column 1 and 2 of table A2.1 the relative ionization cross sections are given at these two electron energies, taken from ref.A10. At both electron energies the Ar ionization cross section is about 3 $Å^2$ (ref. A11). Experimental data on the relative efficiency for some ionization gauges from literature are given in column 3,4 and 5 (ref.A12).

For noble gas ions Boerboom et al. (ref. A13) have measured the gain of an electron multiplier, similar to the one used in our experiment, at ion energies varying between 3 and 90 keV. They observed the gain to be proportional to $\sqrt{E} - \sqrt{E_0}$, where E is the energy of the ion impinging on the multiplier and E_0 is the ion energy at a velocity of 5.5×10^4 msec^{-1}. In our experiment the ion accelerating voltage is 900 V and the voltage across the multiplier 2 kV. The total ion energy is 2900 V.

Neglecting possible differences in the transmission through the ion optics and the mass magnet, one can calculate the overall relative detection efficiency for Ne compared to Ar from table A2.1 (a relative factor .21) and from the above mentioned multiplier gain (a relative factor 1.26). Our measured ratio of intensity for Ne^+ and Ar^+, I_{Ne}/I_{Ar}, thus indicates that no or very little enhancement of the heavier component occurs in the beam; for a 3:1 mixture Ne-Ar we find $I_{Ne}/I_{Ar} = 0.8 - 1.0$, in the onset region.

A 1. K. K. Docken and T. P. Schafer, J. Mol. Spectrosc., *46* (1973) 454
A 2. see e.g. N. Davidson, "Statistical Mechanics", McGraw Hill, New York (1962)
A 3. J. O. Hirschfelder, C. F. Curtiss and R. B. Bird, "Molecular Theory of Gases and Liquids", Wiley, New York (1965)
A 4. Y. Tanaka, K. Yoshino and D. E. Freeman, J. Chem. Phys., *59* (1973) 564
A 5. P. E. Siska, J. M. Parson, T. P. Schafer and Y. T. Lee, J. Chem. Phys., *55* (1971) 5762
A 6. J. D. Poll, private communication
A 7. G. Herzberg, "Molecular Spectra and Molecular Structure", D. v. Nostrand, New York (1954)
A 8. B. N. Srivastava and K. P. Srivastava, J. Chem. Phys., *30* (1969) 984
A 9. C. Y. Ng, Y. T. Lee and J. A. Barker, J. Chem. Phys., *61* (1974) 1996
A10. A. v. Engel, "Ionized Gases", Oxford University Press, London (1965), p. 63
A11. a/ S. Dushman and A. H. Young, Phys. Rev., *68* (1945) 278
b/ Wagener and Johnson, Rev. Sci. Instr., *28* (1951) 278
identical results have been obtained by G. J. Schultz, J. Appl. Phys., *28* (1957) 1149
c/ H. G. Bennewitz and H. D. Dohmann, Vakuum Technik, Heft 1, p.8 (1965)
column 5a in table A2.1 is for a gauge IM IV, Leybold-Hereus
column 5b for a gauge type VM.IR, Hereus.
A12. H. S. W. Massey, E. H. S. Burhop and H. B. Gilbody, "Electronic and Ionic Impact Phenomena", Oxford University Press, London (1969), vol I, p. 128
A13. B. L. Schram, A. J. H. Boerboom, W. Kleine and J. Kistemaker, Physica *32* (1966) 749